



OPEN

PKM2 is a potential prognostic biomarker and related to immune infiltration in lung cancer

Lan Yin^{1,2}, Jiaying Shi^{1,2}, Jingfei Zhang¹, Xinyu Lin¹, Wenhao Jiang¹, Yingchuan Zhu¹, Yue Song¹, Yilu Lu¹ & Yongxin Ma¹✉

Pyruvate kinase M2 (*PKM2*), a subtype of pyruvate kinase, plays a crucial role as a key enzyme in the final step of glycolysis. It is involved in regulating the tumor microenvironment and accelerating tumor progression. However, the relationship between *PKM2* expression and the prognosis and immune infiltration remains unclear in lung cancer. In this study, we analyzed *PKM2* expression in pan-cancer, and investigated its association with prognosis and immune cell infiltration of lung cancer by using multiple online databases, including Gen2, Tumor Immune Estimation Resource (TIMER), Gene Expression Profiling Interactive Analysis (GEPIA), PrognoScan, Kaplan–Meier plotter, and The Human Protein Atlas (HPA). The results showed that *PKM2* expression is elevated in tumor tissues compared with the adjacent normal tissues of most cancers, including lung cancer. Prognostic analysis indicated that high expression of *PKM2* was associated with poorer prognosis in overall lung cancer patients, especially in lung adenocarcinoma (LUAD). Notably, *PKM2* exhibited a strong correlation with B cells and CD4+ T cells in LUAD; and with B cells, CD8+ T cells, CD4+ cells, and macrophages in lung squamous cell carcinoma (LUSC). Furthermore, *PKM2* expression displayed a significant negative correlation with the expression of immune cell markers in both LUAD and LUSC. These findings suggested that *PKM2* could serve as a promising prognostic biomarker for lung cancer and provided insights into its essential role in modulating the immune cell infiltration.

According to the World Health Organization's Global Cancer Observatory (<https://gco.iarc.fr/>), lung cancer has the highest mortality rate in the world, ranking third in terms of incidence. Lung cancer is classified into two main types: small cell lung cancer (SCLC) and non-small cell lung cancer (NSCLC), with approximately 85% of patients diagnosed with NSCLC^{1,2}. Lung adenocarcinoma (LUAD) and lung squamous cell carcinoma (LUSC) are the most common subtypes of NSCLC³. The occurrence and progression of NSCLC involve a dynamic and intricate process closely linked to the tumor microenvironment, where immune cells can significantly impact cancer cell growth and development⁴. Therefore, there is an urgent need to identify a new therapeutic target associated with the prognosis and immune infiltration of lung cancer.

PKM2, a subtype of pyruvate kinase, is highly expressed in proliferating and tumor cells⁵. *PKM2* predominantly exists in the form of monomer and dimer, functioning as a crucial rate-limiting enzyme in glycolysis and a significant regulator of tumor metabolism^{6,7}. Its enzyme activity is intricately regulated, enabling cells to adapt to diverse physiological states⁸. Recent research has increasingly focused on the role of *PKM2* as a vital regulator of cellular pathological and physiological activities in autoimmune responses and inflammatory processes⁹. Studies have shown that *PKM2* could modulate the formation of T cell subpopulations and affect T cell metabolism, while also exerting regulatory effects on B cells, dendritic cells, and tumor-associated macrophages¹⁰. Notably, dimerized *PKM2* has been reported to bind to the promoter of Programmed Cell Death-Ligand 1 (PD-L1), resulting in a significant increase of PD-L1 expression, thereby facilitating immune evasion by cancer cells¹¹. Wang et al. have proposed that exosomal *PKM2* may serve as a promising biomarker and therapeutic target for cisplatin resistance in NSCLC¹². However, the precise function and mechanism of *PKM2* in the progression of lung cancer remain elusive.

In this study, we conducted a comprehensive analysis of *PKM2* expression and its correlation with prognosis in various tumor types. The mRNA expression levels of *PKM2* in tumors and adjacent normal tissues of the LUAD and LUSC were compared using the Kaplan–Meier plotter. Additionally, the protein expression levels of *PKM2* were examined using The Human Protein Atlas (HPA) database. Furthermore, we systematically investigated

¹Department of Medical Genetics, West China Hospital, Sichuan University, Chengdu, China. ²These authors contributed equally: Lan Yin and Jiaying Shi. ✉email: mayongxin@gmail.com

the relationship between *PKM2* expression and immune infiltration in these two subtypes of NSCLC. Our findings revealed that *PKM2* is significantly upregulated in lung cancer and can serve as a valuable biomarker for prognostic prediction. Moreover, our results suggested that *PKM2* may modulate tumor immunity by regulating immune cell infiltration in NSCLC.

Results

The mRNA expression levels of *PKM2* in pan-cancer

Figure 1A illustrates the widespread upregulation of *PKM2* in tumors compared with adjacent normal tissues across various cancer types (all $p < 0.05$) in the Gent2 database (GPL96 platform). However, *PKM2* was downregulated in heart and skin cancer tissues ($p < 0.05$). Next, we used TIMER to verify the differential expression of *PKM2* in pan-cancer. With the exception of prostate adenocarcinoma (PRAD), where *PKM2* expression was higher in adjacent normal tissues than in tumor tissues, other cancers exhibited overexpression of *PKM2* in tumor tissues (Fig. 1B). In addition, we investigated the mRNA expression levels of *PKM2* in tumors and adjacent normal tissues from the TCGA and GTEx datasets using GEPIA database (Fig. 1C). The results revealed higher *PKM2* mRNA levels in breast invasive carcinoma (BRCA), cervical squamous cell carcinoma and endocervical adenocarcinoma (CESC), cholangio carcinoma (CHOL), colon adenocarcinoma (COAD), lymphoid neoplasm diffuse large B-cell lymphoma (DLBC), kidney renal clear cell carcinoma (KIRC), kidney renal papillary cell carcinoma (KIRP), liver hepatocellular carcinoma (LIHC), LUSC, ovarian serous cystadenocarcinoma (OV), pancreatic adenocarcinoma (PAAD), rectum adenocarcinoma (READ), skin cutaneous melanoma (SKCM), stomach adenocarcinoma (STAD), uterine corpus endometrial carcinoma (UCEC) and uterine carcinosarcoma (UCS) than in adjacent normal tissues (all $p < 0.05$). However, no statistical differences in the expression of *PKM2* were observed between tumor and adjacent normal tissues in other tumors.

Analysis of the prognostic value of *PKM2* in human cancer

The prognostic value of *PKM2* in cancers was evaluated using GEPIA and PrognScan databases. In the GEPIA database, high expression of *PKM2* was associated with worse OS in CESC, head and neck squamous cell carcinoma (HNSC), acute myeloid leukemia (LAML), LIHC, LUAD, mesothelioma (MESO), PAAD, and uveal melanoma (UVM), but was associated with a better OS in KIRC (Fig. 2A; Table S1). In addition, high expression of *PKM2* was negatively associated with disease-free survival (DFS) in glioblastoma multiforme (GBM), MESO, PAAD, and UVM (Fig. 2B). Similarly, *PKM2* expression was shown to be negatively correlated with the prognosis of 8 out of 12 cancers (cox $p < 0.05$), including blood, brain, breast, colorectal, eye, lung, prostate, and soft-tissue cancers (Fig. 2C).

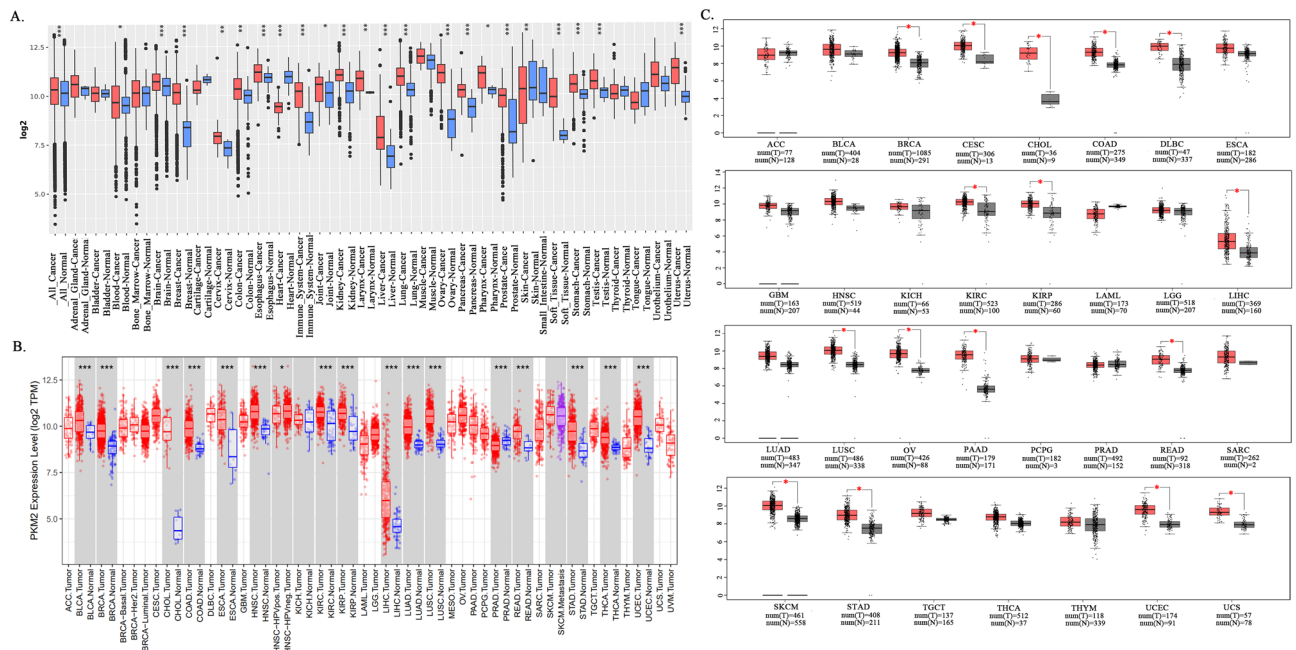


Figure 1. Analysis of *PKM2* expression levels in pan-cancer. (A) Comparison of the expression level of *PKM2* in tumors and adjacent normal tissues in pan-cancer using the Gent2 database. (B) The expression level of *PKM2* in different cancers and adjacent normal tissues in the TIMER database. (C) The expression levels of *PKM2* in different cancers and adjacent normal tissues were compared using the GEPIA database. (* $p < 0.05$, ** $p < 0.01$, *** $p < 0.001$).

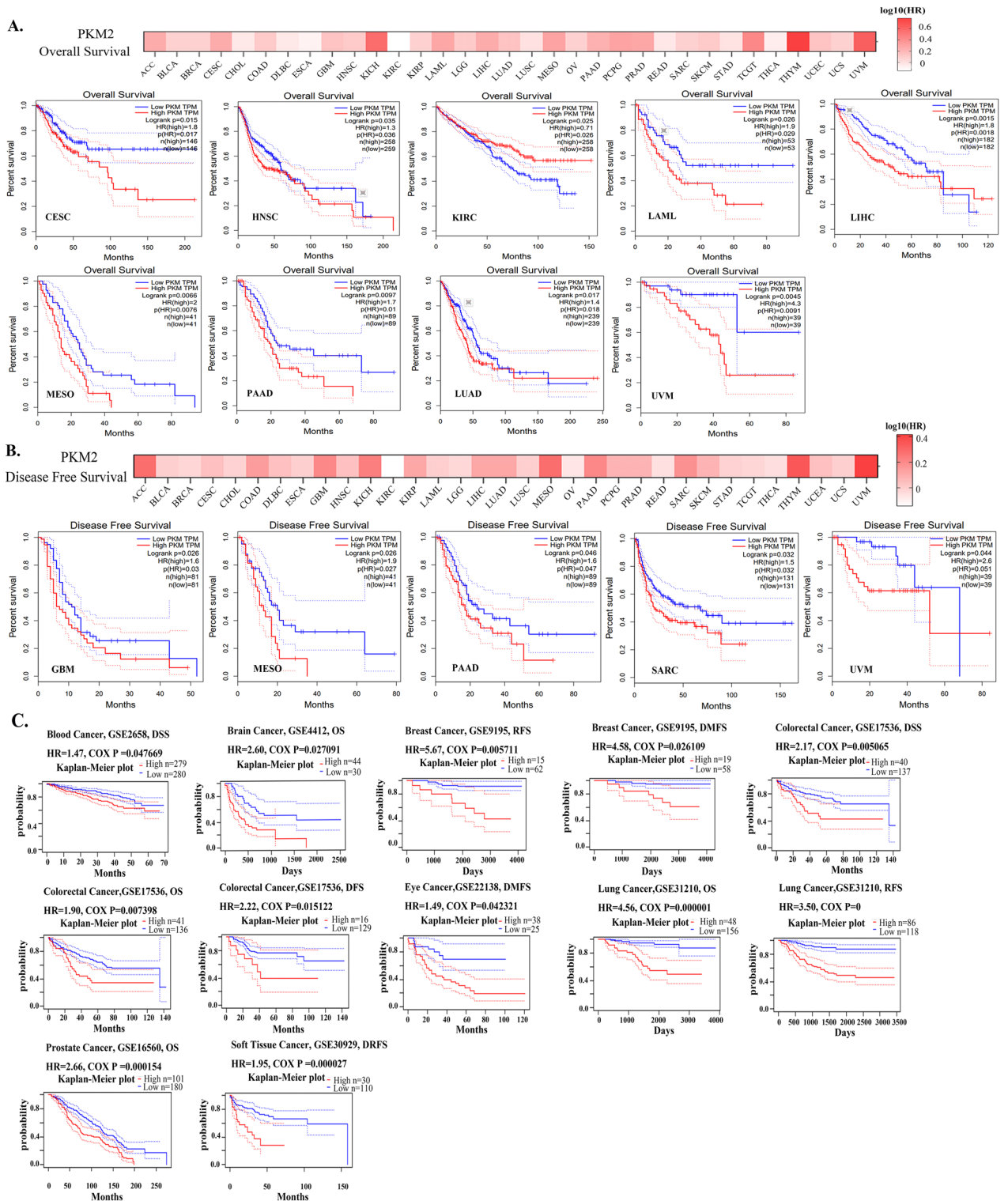


Figure 2. Analysis of the prognostic significance of *PKM2* in different types of cancers. The relationship between *PKM2* expression and overall survival (A) and disease-free survival (B) in different cancers was analyzed by GEPIA database. (C) The prognostic value of *PKM2* in different cancers was analyzed using the Prognoscan database.

Expression analysis of *PKM2* in lung cancer

Given the exceptionally high global mortality rate and the third-highest incidence rate of lung cancer, we focused towards exploring the potential role of *PKM2* as a biomarker in lung cancer in our subsequent research. The

differential expression of *PKM2* in lung cancer was verified using the KM plotter database. Both the RNA-seq based data (Fig. 3A) and the gene chip-based data (Fig. 3B) demonstrated that *PKM2* mRNA expression levels were higher in tumor tissues compared to adjacent normal tissues, regardless of whether non-paired or paired samples were used as controls. Meanwhile, we analyzed the expression of *PKM2* at different stages of LUAD and LUSC using the GEPIA database. The results indicated significant variations in *PKM2* expression levels across different stages in LUAD ($\text{Pr}(> F) < 0.05$; Fig. 3C). Subsequently, we confirmed the protein expression of *PKM2* in LUAD and LUSC by immunohistochemistry analysis in the HPA database. The findings revealed elevated protein levels of *PKM2* in both LUAD and LUSC tumor tissues compared to paired adjacent normal tissues (Fig. 3D,E).

Association of *PKM2* expression with prognosis and clinical characteristics of lung cancer patients

The effect of *PKM2* expression on prognosis of lung cancer patients was further determined using the KM plotter database. The results of gene chip-based data showed that high expression of *PKM2* was associated with poor

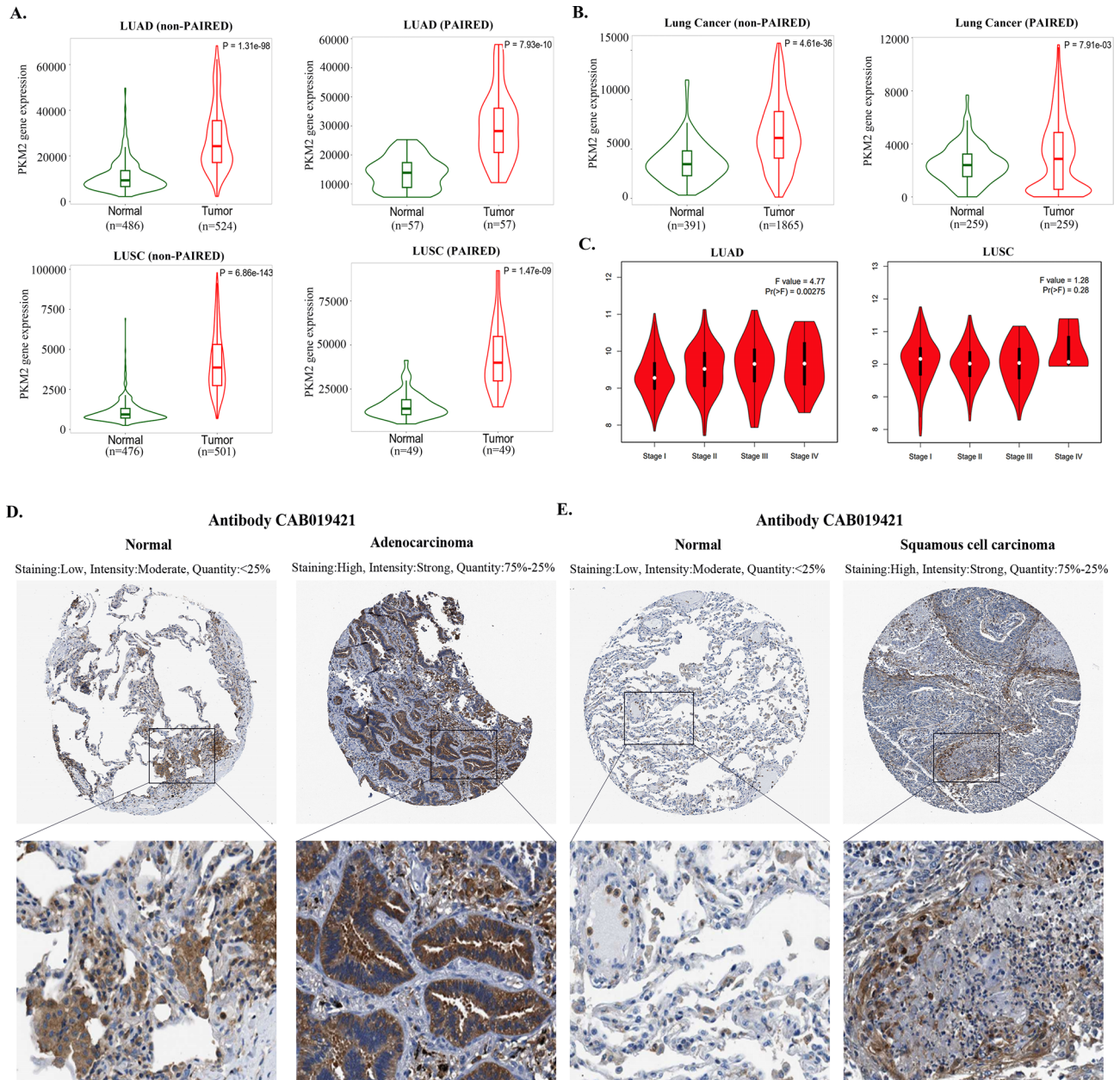


Figure 3. Analysis of the mRNA and protein expression levels of *PKM2* in tumor and adjacent normal tissues of lung cancer. RNA-seq (A) and gene chip (B) data from the KM plotter database were used to compare the expression levels of *PKM2* in tumor and adjacent normal tissues. (C) Correlation between *PKM2* expression and tumor stage in LUAD and LUSC (GEPIA database). (D) *PKM2* protein expression levels in tumors and adjacent normal tissues of LUAD and LUSC patients were detected by immunohistochemistry in the HPA database.

OS (HR = 1.56, $p = 3e-13$), the first progression (FP, HR = 1.97, $p = 5.9e-15$), and post progression survival (PPS, HR = 1.3, $p = 0.041$) in lung cancer patients (Fig. 4A). However, the analysis of RNA-seq based data showed that high expression of *PKM2* only correlated with poor OS (HR = 1.75, $p = 0.00015$) in LUAD, and it was not associated with relapse-free survival (RFS) in LUAD or OS and RFS in LUSC (Fig. 4B). These findings suggested that *PKM2* expression has prognostic value for overall lung cancer, while its association with prognosis is specific to LUAD among the two most common subtypes of NSCLC.

Meanwhile, we examined the relationship between *PKM2* expression and various clinical characteristics of lung cancer using the KM plotter database. As demonstrated in Table 1, high expression of *PKM2* had a detrimental effect on OS, FP, and PPS in specific subgroups, including females (OS: HR = 1.69, $p = 2.4e-06$; FP: HR = 2.5, $p = 3.8e-11$; PPS: HR = 1.57, $p = 0.017$), LUAD patients (OS: HR = 2.64, $p = 1.1e-15$; FP: HR = 2.36, $p < 1E-16$; PPS: HR = 1.41, $p = 0.03$), stage 1 patients (OS: HR = 2.38, $p = 5.9e-12$; FP: HR = 2.18, $p = 0.00042$; PPS: HR = 2.52, $p = 0.0065$), AJCC_N1 (OS: HR = 1.54, $p = 0.01$; FP: HR = 2.62, $p = 1e-05$; PPS: HR = 1.72, $p = 0.016$), non-smokers (OS: HR = 4.56, $p = 3.1e-06$; FP: HR = 3.72, $p = 2.6e-07$; PPS: HR = 2.31, $p = 0.0081$), and patients with negative surgical margins (OS: HR = 3.03, $p = 2.1e-15$; FP: HR = 4.8, $p = 2.2e-16$; PPS: HR = 1.51, $p = 0.0057$).

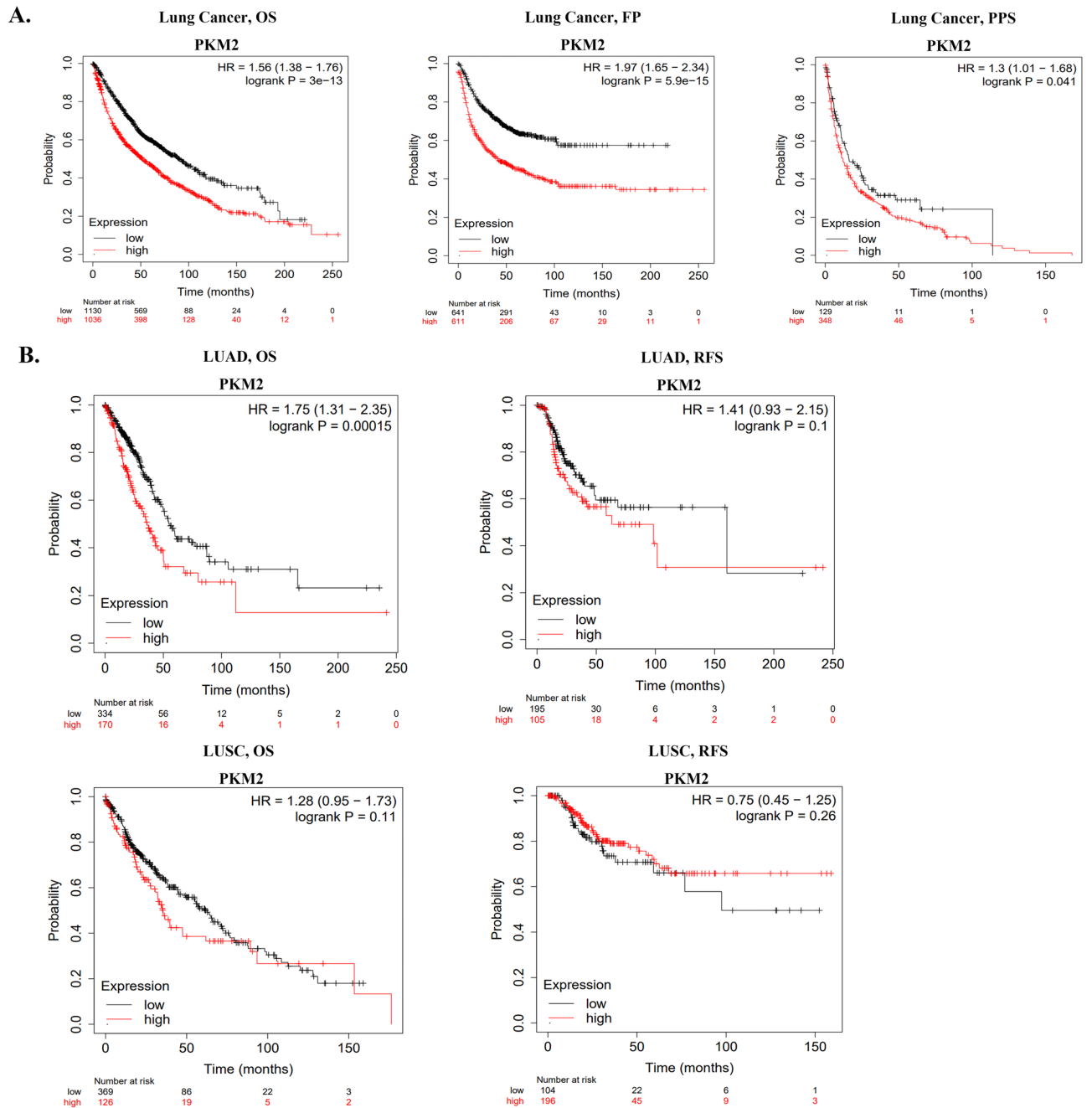


Figure 4. Survival curves for *PKM2* in lung cancer using the Kaplan–Meier plotter database. (A) OS, FP, and PPS of lung cancer based on the gene chip data. High expression of *PKM2* was correlated with poor OS, FP and PPS. (B) OS and RFS of LUAD and LUSC based on the RNA-seq data.

Clinicopathological factors	Overall survival			First progression			Post progression survival		
	N	Hazard ratio	<i>p</i> value	N	Hazard ratio	<i>p</i> value	N	Hazard ratio	<i>p</i> value
Gender									
Female	808	1.69 (1.35–2.1)	2.4e–06	500	2.5 (1.89–3.31)	3.8e–11	193	1.57 (1.08–2.29)	0.017
Male	1247	1.69 (1.4–2.06)	6.4e–08	752	1.75 (1.41–2.18)	3.2e–07	284	1.28 (0.92–1.78)	0.15
Histology									
Adenocarcinoma	1161	2.64 (2.06–3.38)	1.1e–15	906	2.36 (1.93–2.89)	<1E–16	376	1.41 (1.03–1.92)	0.03
Squamous cell carcinoma	780	1.36 (1.12–1.65)	0.0021	220	1.47 (0.97–2.22)	0.067	51	1.32 (0.74–2.37)	0.34
Stage									
1	656	2.38 (1.85–3.07)	5.9e–12	325	2.18 (1.4–3.4)	0.00042	78	2.52 (1.27–5.02)	0.0065
2	392	2.08 (1.5–2.88)	6.3e–06	130	1.23 (0.73–2.06)	0.44	58	2.16 (1.12–4.15)	0.019
3	108	1.26 (0.76–2.08)	0.37	19	–	–	10	–	–
4	4	–	–	0	–	–	0	–	–
AJCC_T									
T1	429	2.03 (1.46–2.83)	1.8e–05	338	3.08 (1.94–4.89)	4.8e–07	111	0.66 (0.42–1.03)	0.068
T2	578	1.31 (1.03–1.67)	0.025	415	1.46 (1.12–1.92)	0.0054	221	1.32 (0.95–1.83)	0.095
T3	82	1.57 (0.93–2.63)	0.087	48	2.08 (1.01–4.3)	0.044	35	0.85 (0.41–1.75)	0.66
T4	43	0.6 (0.31–1.17)	0.13	25	0.36 (0.1–1.22)	0.087	17	–	–
AJCC_N									
N0	768	1.47 (1.17–1.86)	0.00095	562	1.53 (1.16–2.02)	0.0022	218	0.87 (0.63–1.21)	0.41
N1	253	1.54 (1.11–2.15)	0.01	181	2.62 (1.68–4.09)	1e–05	105	1.72 (1.1–2.7)	0.016
N2	104	1.12 (0.74–1.7)	0.58	76	0.7 (0.39–1.26)	0.23	55	0.6 (0.34–1.06)	0.078
AJCC_M									
M0	682	1.45 (1.18–1.79)	0.00038	464	1.26 (0.93–1.71)	0.13	159	1.16 (0.82–1.64)	0.41
M1	10	–	–	6	–	–	4	–	–
Grade									
I	188	1.34 (0.89–2.02)	0.17	136	0.7 (0.43–1.14)	0.15	88	1.93 (1.2–3.1)	0.0058
II	302	1.86 (1.31–2.63)	0.00043	166	1.45 (0.97–2.17)	0.07	106	1.4 (0.89–2.18)	0.14
III	75	3.11 (1.58–6.14)	0.00057	52	0.54 (0.22–1.3)	0.16	28	0.25 (0.07–0.89)	0.021
Smoking history									
Yes	833	1.72 (1.39–2.12)	4.6e–07	584	1.97 (1.54–2.52)	4.4e–08	266	1.28 (0.94–1.75)	0.12
No	204	4.56 (2.27–9.16)	3.1e–06	190	3.72 (2.18–6.36)	2.6e–07	70	2.31 (1.22–4.35)	0.0081
Chemotherapy									
Yes	173	1.97 (1.29–2.99)	0.0013	122	1.67 (1.04–2.69)	0.032	88	2.06 (1.25–3.37)	0.0036
No	400	1.63 (1.22–2.19)	0.00095	285	1.29 (0.87–1.92)	0.2	153	1.43 (0.92–2.23)	0.11
Radiotherapy									
Yes	65	2.74 (1.51–4.99)	6e–04	62	1.51 (0.81–2.82)	0.19	54	2.02 (1.08–3.77)	0.025
No	363	1.24 (0.92–1.67)	0.16	289	0.97 (0.7–1.35)	0.87	163	1.12 (0.78–1.6)	0.53
Surgery success									
Only surgical margins negative	704	3.03 (2.27–4.04)	2.1e–15	558	4.8 (3.18–7.26)	2.2e–16	276	1.51 (1.13–2.04)	0.0057

Table 1. Analysis of the correlation between PKM2 mRNA expression and prognosis of different clinicopathologic factors in lung cancer by Kaplan–Meier plotter. Bold values indicate $p < 0.05$.

In addition, high *PKM2* expression correlated with poor OS and PFS in males (OS: HR = 1.69, $p = 6.4e-08$; FP: HR = 1.75, $p = 3.2e-07$), AJCC (American joint committee on cancer)_T1 patients (OS: HR = 2.03, $p = 1.8e-05$; FP: HR = 3.08, $p = 4.8e-07$), AJCC_T2 patients (OS: HR = 1.31, $p = 0.025$; FP: HR = 1.46, $p = 0.0054$), AJCC_N0 patients (OS: HR = 1.47, $p = 0.00095$; FP: HR = 1.53, $p = 0.0022$), and patients with a history of smoking (OS: HR = 1.72, $p = 4.6e-07$; FP: HR = 1.97, $p = 4.4e-08$). These findings highlight the prognostic significance of *PKM2* expression in different clinical characteristics of lung cancer patients, particularly in localized and regional early and mid-stage cancers.

Correlation of *PKM2* expression with the level of infiltrating immune cells in LUAD and LUSC
Subsequently, we investigated the association between *PKM2* expression and immune cell infiltration in LUAD and LUSC using the TIMER database. As displayed in Fig. 5A and B, the *PKM2* expression levels were positively correlated with the tumor purity (the proportion of cancer cells in a sample) in LUAD and LUSC. The expression level of *PKM2* was significantly negatively correlated with the infiltration levels of B cells (partial. $cor = -0.312$, $p = 2.33e-12$) and CD4+ T cells (partial. $cor = -0.113$, $p = 1.25e-02$) in LUAD. Similarly, in LUSC, *PKM2* expression exhibited a significant negative correlation with the infiltration levels of B cells

(partial. $cor = -0.195$, $p = 1.92e-05$), CD8+ T cells (partial. $cor = -0.156$, $p = 6.62e-04$), CD4+ T cells (partial. $cor = -0.169$, $p = 2.22e-04$), and macrophages (partial. $cor = -0.094$, $p = 4.05e-02$). These findings highlight the regulatory role of *PKM2* expression in modulating the infiltration of immune cells in LUAD and LUSC.

Analysis of the correlation between *PKM2* mRNA levels and markers of different immune cell subsets

Then, we explored the correlation between *PKM2* mRNA levels and markers of different subsets of immune cells in LUAD and LUSC using TIMER and GEPIA databases¹³. Using TIMER database, purity adjustments were made for correlation analyses given that tumor purity of clinical samples would affect the analysis of immune infiltration (Table 2). In LUAD, *PKM2* expression was negatively correlated with the expression of specific immune cell markers (Fig. 6A–E), including markers of CD8+ T cells, T cells (general), B cells, neutrophils, and DCs. Moreover, *PKM2* expression has a significantly negative correlation with the expression of marker genes of different T cells subsets in LUAD (Fig. 6G–I), such as markers of Treg, Th1 and exhausted T cells. However, a significant positive correlation between *PKM2* and the markers of TAM was observed (Fig. 6F). In LUSC, *PKM2* expression was negatively correlated with the expression of markers of CD8+ T cells, T cells (general), B cells, M1 macrophage, DCs, neutrophils, monocyte, and NK cells (Fig. 6J–Q). Similarly, a negative correlation was observed between *PKM2* expression and different subsets of T cells, including Th2, Treg, Th1, T cell exhaustion, and Tfh (Fig. 6R–V). However, *PKM2* expression had a significant positive correlation with PTGS2 ($r = 0.119$, $p = 0.009$), a marker of M1 Macrophage, STAT3 ($r = 0.114$, $p = 0.013$), a marker of Th17, and TGF β ($r = 0.241$, $p = 9.85e-08$), a marker of Treg (Table 2). Table 3 shows the correlation analysis between *PKM2* mRNA levels and marker genes of different immune cells in GEPIA database. Collectively, *PKM2* expression was significantly correlated with the expression of marker genes from tumor-infiltrating CD8+ T cells, T cells (general), B cells, Neutrophils, DCs, Th1, Th2, Th17, Tfh, Treg, and depleted T cells both in LUAD and LUSC. Our findings implied a critical role of *PKM2* in tumor immune infiltration in LUAD and LUSC.

Discussion

PKM2 has been shown to be upregulated in various types of cancers and plays a crucial role in cancer metabolism⁶. Its functions extend beyond the regulation of glucose metabolic, as it has also been implicated in the modulation of intracellular reactive oxygen species levels and the maintenance of amino acid balance^{14–16}. In addition, emerging evidence suggests that *PKM2* could function as a protein kinase, mediating cancer progression, chemical resistance, and immunity regulation^{17–19}.

Recent studies have demonstrated that *PKM2* is highly expressed in multiple cancers, and is closely associated with the disease progression, such as in pancreatic ductal adenocarcinoma (PDAC)²⁰, colorectal cancer²¹, breast cancer²², and hepatocellular cancer²³. In brain tumors, various findings demonstrated that in addition to its key role as a core regulator of cellular glycolysis, *PKM2* holds a critical tumorigenic function as a protein kinase in the nucleus through its involvement in gene transcription and as a transcriptional co-activator of oncogenic signals²⁴. Moreover, in bladder cancer (BCa), *PKM2* has been found to promote the growth, migration, and cisplatin resistance of BCa cells and may serve as a poor prognostic factor for BCa patients²⁵. In our study, we found that *PKM2* mRNA expression levels were significantly upregulated in most human tumors using the GenT2, TIMER,

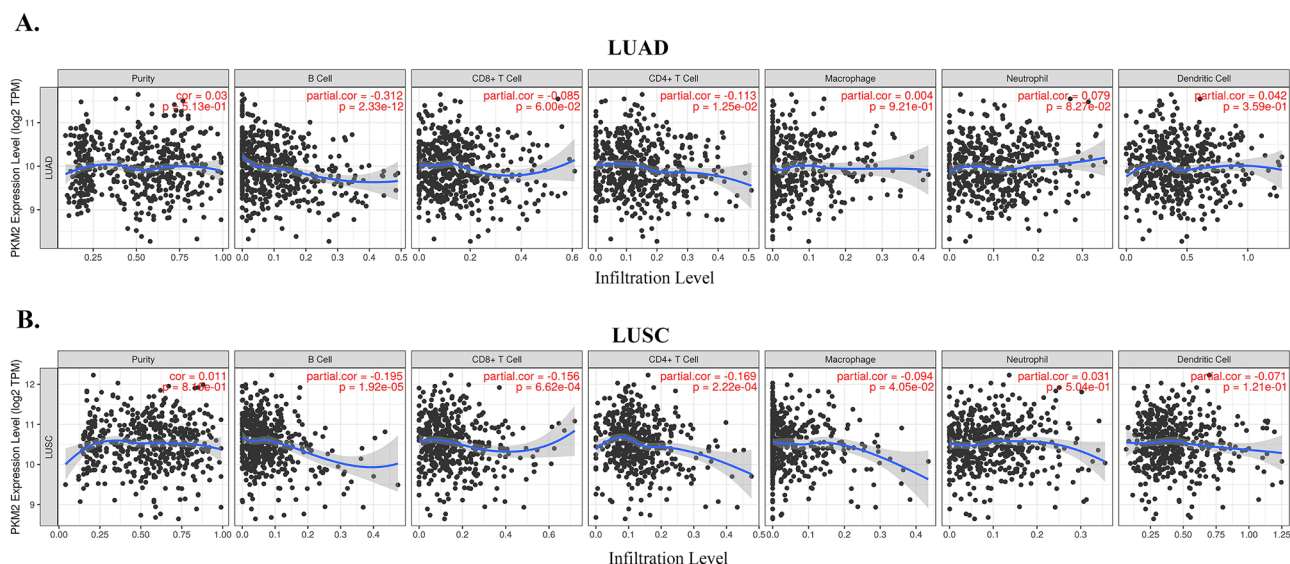


Figure 5. Correlation analysis of *PKM2* expression and infiltration levels of immune cells in LUAD and LUSC tissues using the TIMER database. (A) In LUAD, *PKM2* was positively correlated with tumor purity and negatively correlated with the infiltration levels of B-cells and CD4+ T cells. (B) *PKM2* expression in LUSC was positively correlated with tumor purity and negatively correlated with infiltration levels of B cells, CD8+ T cells, CD4+ T cells, and macrophages.

Description	Gene markers	LUAD				LUSC			
		None		Purity		None		Purity	
		Core	<i>p</i>	Core	<i>p</i>	Core	<i>p</i>	Core	<i>p</i>
CD8+ T cell	CD8A	-0.150	**	-0.157	***	-0.224	***	-0.237	***
	CD8B	-0.166	***	-0.166	***	-0.259	***	-0.259	***
T cell (general)	CD3D	-0.157	***	-0.173	***	-0.208	***	-0.227	***
	CD3E	-0.191	***	-0.217	***	-0.204	***	-0.225	***
	CD2	-0.186	***	-0.208	***	-0.210	***	-0.226	***
B cell	CD19	-0.275	***	-0.306	***	-0.257	***	-0.307	***
	CD79A	-0.240	***	-0.261	***	-0.191	***	-0.232	***
Monocyte	CD86	0.021	0.629	0.042	0.353	-0.138	**	-0.147	**
	CSF1R	0.076	0.084	0.100	*	-0.036	0.424	-0.023	0.618
TAM	CCL2	0.047	0.288	0.064	0.155	-0.014	0.756	-0.014	0.759
	CD68	0.131	**	0.153	***	0.060	0.182	0.067	0.142
	IL10	-0.054	0.224	-0.044	0.330	-0.085	0.058	-0.097	*
M1 Macrophage	NOS2	-0.032	0.464	-0.032	0.482	-0.131	**	-0.133	**
	IRF5	0.005	0.910	0.007	0.882	-0.012	0.792	-0.003	0.944
	PTGS2	0.074	0.095	0.076	0.092	0.119	**	0.119	**
M2 Macrophage	CD163	0.075	0.090	0.100	*	-0.025	0.575	-0.013	0.779
	VSIG4	0.054	0.217	0.067	0.137	-0.021	0.646	-0.009	0.845
	MS4A4A	-0.020	0.645	-0.005	0.909	-0.100	*	-0.097	*
Neutrophils	CD66b	-0.193	***	-0.198	***	-0.098	*	-0.099	*
	CD11b	0.055	0.216	0.077	0.089	-0.051	0.257	-0.041	0.376
	CCR7	-0.235	***	-0.264	***	-0.239	***	-0.265	***
Natural killer cell	KIR2DL1	-0.057	0.197	-0.059	0.190	-0.052	0.246	-0.056	0.223
	KIR2DL3	0.073	0.098	0.079	0.080	-0.141	**	-0.127	**
	KIR2DL4	0.098	*	0.100	*	-0.051	0.255	-0.043	0.353
	KIR3DL1	-0.023	0.605	-0.030	0.504	-0.072	0.106	-0.061	0.180
	KIR3DL2	-0.023	0.598	-0.016	0.727	-0.146	**	-0.148	**
	KIR3DL3	0.061	0.165	0.058	0.195	0.013	0.769	0.003	0.948
Dendritic cell	KIR2DS4	-0.005	0.902	-0.009	0.845	-0.056	0.207	-0.058	0.205
	HLA-DPB1	-0.166	***	-0.167	***	-0.131	**	-0.140	**
	HLA-DQB1	-0.111	*	-0.107	*	-0.100	*	-0.100	**
	HLA-DRA	-0.133	**	-0.131	**	-0.132	**	-0.138	**
	HLA-DPA1	-0.135	**	-0.131	**	-0.143	**	-0.151	***
	ITGAX	-0.016	0.710	-0.009	0.837	-0.119	**	-0.135	**
	NRP1	0.013	0.768	0.005	0.904	0.071	0.110	0.082	0.0754
Th1	CD1C	-0.217	***	-0.220	***	-0.097	*	-0.103	*
	T-bet	-0.125	**	-0.137	**	-0.240	***	-0.258	***
	STAT4	-0.112	*	-0.121	**	-0.159	***	-0.177	***
	STAT1	0.109	*	0.122	**	-0.049	0.276	-0.056	0.225
	IFN- γ	-0.021	0.637	-0.015	0.735	-0.149	**	-0.155	**
	TNF- α	-0.020	0.645	-0.009	0.837	0.084	0.059	0.087	0.058
Th2	GATA3	0.012	0.792	0.031	0.494	0.011	0.809	0.015	0.742
	STAT6	-0.050	0.256	-0.055	0.222	-0.038	0.394	-0.042	0.359
	STAT5A	-0.084	0.056	-0.079	0.078	-0.160	***	-0.168	***
	IL13	-0.092	*	-0.086	0.057	-0.133	**	-0.146	**
Tfh	BCL6	-0.057	0.196	-0.061	0.178	-0.106	*	-0.116	*
	IL21	-0.007	0.869	-0.004	0.931	-0.168	***	-0.160	***
Th17	STAT3	-0.067	0.129	-0.066	0.142	0.112	*	0.114	*
	IL17A	-0.083	0.059	-0.093	*	-0.074	0.099	-0.074	0.105
Treg	FOXP3	-0.035	0.424	-0.032	0.477	-0.124	**	-0.127	**
	CCR8	-0.084	0.057	-0.080	0.078	-0.125	**	-0.132	**
	STAT5B	-0.209	***	-0.207	***	-0.181	***	-0.179	***
	TGF β	0.061	0.166	0.069	0.128	0.235	***	0.241	***

Continued

Description	Gene markers	LUAD				LUSC			
		None		Purity		None		Purity	
		Core	<i>p</i>	Core	<i>p</i>	Core	<i>p</i>	Core	<i>p</i>
T cell exhaustion	PD-1	-0.036	0.420	-0.035	0.436	-0.237	***	-0.256	***
	CTLA4	-0.116	**	-0.123	**	-0.245	***	-0.271	***
	LAG3	0.003	0.949	0.019	0.677	-0.175	***	-0.178	***
	TIM-3	0.041	0.355	0.061	0.177	-0.111	*	-0.113	*
	GZMB	0.075	0.087	0.090	*	-0.184	***	-0.196	***

Table 2. Correlation analysis of PKM2 with immune cell-related genes and markers. *Cor* R value of Spearman's correlation, *None* correlation without adjustment, *Purity* correlation adjusted by purity. * $p < 0.05$, ** $p < 0.01$, *** $p < 0.001$.

and GEPIA databases. However, the expression of *PKM2* varied across different types of cancer, which could be attributed to variations in data collection methods and underlying pathogenic mechanisms¹³. Notably, tumor tissues consistently exhibited higher levels of *PKM2* expression compared to controls in lung cancer. High *PKM2* expression has been associated with poorer prognosis in various cancer types, including lung cancer, as revealed by survival analysis in the GEPIA and Prognoscan databases. Combining the findings from both databases, it became evident that high *PKM2* expression is detrimental to the prognosis of lung cancer patients.

As previously reported, *PKM2* expression could drive the metabolic reprogramming, promote proliferation, and induce glycolytic metabolism of NSCLC^{26,27}. Additionally, *PKM2* has been implicated in promoting invasion and epithelial-mesenchymal transition (EMT) in lung cancer²⁸. Our analysis, encompassing RNA-seq and gene chip data from both paired and unpaired cancer and normal tissues, consistently revealed higher *PKM2* expression in lung cancer at both protein and mRNA levels. Furthermore, Kaplan–Meier Plotter analyses confirmed a significant correlation between high *PKM2* expression and a worse prognosis in lung cancer, particularly in localized and regional early and mid-stage cancers. Collectively, these findings underscore the potential of *PKM2* as a prognostic biomarker for lung cancer.

The composition and activity of infiltrating immune cells within the tumor microenvironment play a crucial role in shaping the immune response and have significant implications for the clinical prognosis of cancer patients²⁹. Hou et al.³⁰ and Li et al.²³ have demonstrated that *PKM2* can drive hepatocellular carcinoma progression by inducing macrophage differentiation and inducing an immunosuppressive microenvironment. Our study demonstrated that *PKM2* expression was negatively correlated with B cells and CD4+ cells in LUAD and had a strong negative correlation with B cells, CD4+ and CD8+ T cells, and macrophages in LUSC. These findings suggest that *PKM2* plays a pivotal role in regulating tumor immunity in lung cancer, thereby influencing the prognosis of the patients. Previous studies have reported the presence of tumor-antagonizing immune cells within the tumor microenvironment, including CD8+ cells, natural killer (NK) cells, DCs, M1 macrophages, and neutrophils³¹. Our analysis revealed a significant negative correlation between *PKM2* expression and markers of CD8+ T cells, neutrophils, and DCs in both LUAD and LUSC. Moreover, in LUSC, *PKM2* was also negatively correlated with the expression of the M1 macrophage markers, NOS2 and PTGS2, and NK cell markers, KIR2DL3 and KIR3DL2. These results suggest that elevated *PKM2* expression may contribute to the progression of LUAD and LUSC by impeding the infiltration of tumor-antagonizing immune cells.

Previous studies have highlighted the nonmetabolic role of *PKM2* in modulating Th17 cell differentiation and function in autoimmune-mediated inflammation through enhanced STAT3 activation¹⁷. Our findings revealed a positive correlation between *PKM2* expression and STAT3, a marker for Th17 cells, in LUSC. Additionally, *PKM2* expression also showed correlations with markers of various subsets of T helper (Th) cells, including Th1 (T-bet, STAT4, and IFN- γ), Th2 (STAT5A and IL13), Tfh (BCL6 and IL-21), and Tregs (FOXP3, CCR8, STAT5B, and TGF- β). In contrast, in LUAD, *PKM2* expression exhibited a significant negative correlation with markers of Th1 cells (T-bet, STAT4, and STAT1) and Treg cells (STAT5B). These results suggest a role for *PKM2* in regulating tumor-infiltration of T-helper cells. Interestingly, *PKM2* expression was also negatively correlated with markers of exhausted T cells especially in LUSC, where the expression of inhibitory immune checkpoint proteins PD-1, CTLA4, LAG3, and TIM-3³² were also negatively correlated with *PKM2* expression. Many cancers evade the immune response by overexpressing inhibitory ligands to suppress T-cell function, thereby promoting their own progression³³. Accordingly, we speculated that this could explain the high expression of *PKM2* in LUSC tumor tissues despite its lack of close association with the prognosis of LUSC.

However, it is essential to acknowledge that our study has limitations due to its reliance on public resource databases. Nevertheless, the consistent findings across multiple databases substantiate the potential of *PKM2* as a prognostic biomarker for lung cancer and as an indicator of immune cell infiltration levels in LUAD and LUSC.

In conclusion, our study established a clear association between elevated *PKM2* expression and unfavorable prognosis in lung cancer patients, particularly those with localized and regional early and mid-stage lung cancers, by integrating data from multiple databases. More importantly, our study unveiled a correlation between *PKM2* and immune infiltration in lung cancer, providing novel insights for the treatment of lung cancer patients. Our study highlights the potential of *PKM2* as a promising therapeutic target in lung cancer.

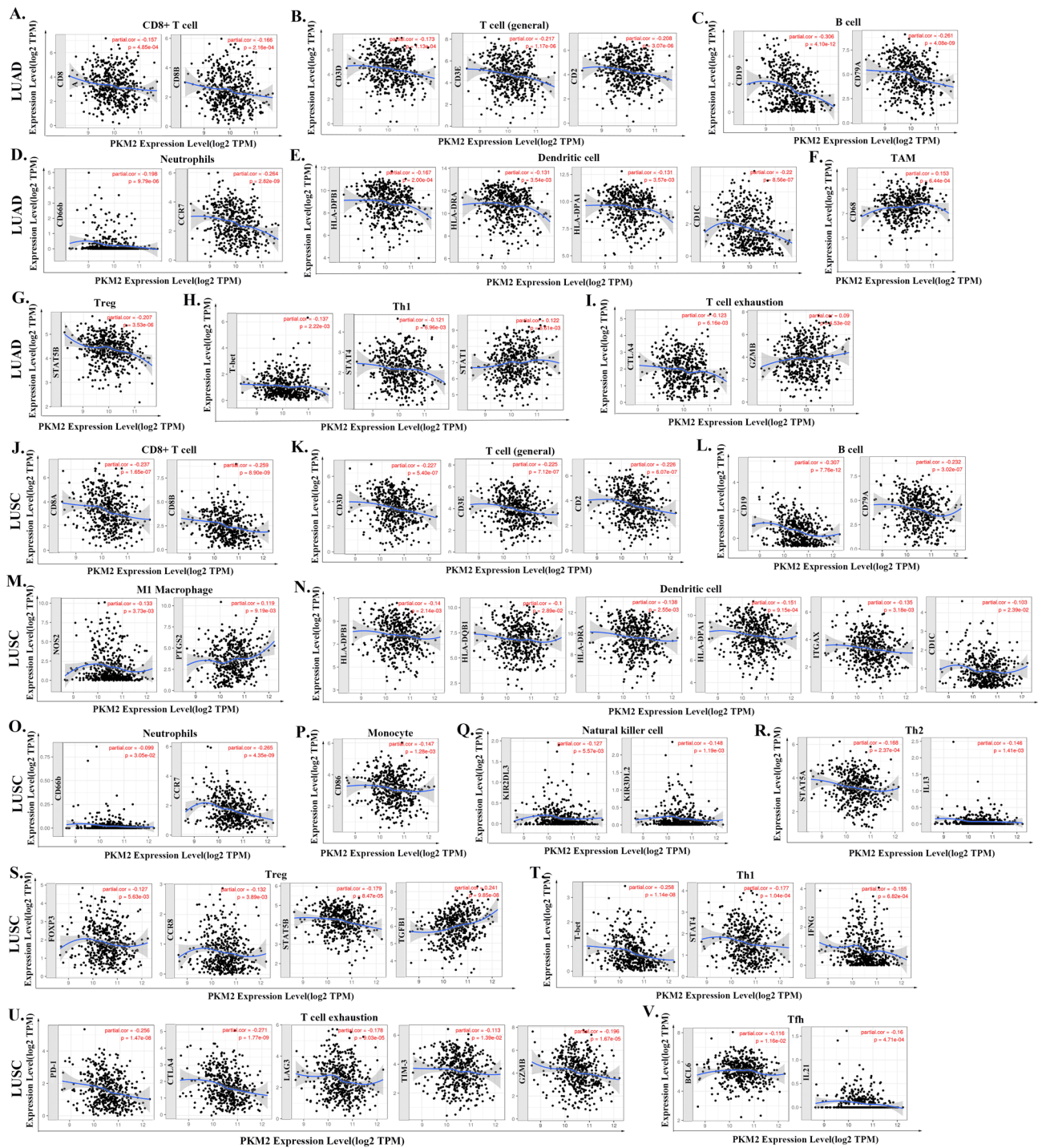


Figure 6. The correlation between *PKM2* expression and levels of infiltrating immune cell markers in LUAD (A–I) and LUSC (J–V) was analyzed using the TIMER database. In LUAD, (A–I) show the correlation between *PKM2* expression and the marker genes in LUAD of CD8+ T cell (CD8A and CD8B) (A), T cell (general) (CD3D, CD3E and CD2) (B), B cell (CD19 and CD79A) (C), Neutrophils (CD66b and CCR7) (D), DCs (HLA-DPB1, HLA-DRA, HLA-DPA1, and CD1C) (E), TAM (CD68) (F), Treg (STAT5B) (G), Th1 (T-bet, STAT4, and STAT1) (H), and T cell exhaustion (CTLA4 and GZMB) (I). In LUSC, (J–V) show the correlations between *CCL14* expression and the marker genes of CD8+ T cell (CD8A and CD8B) (J), T cell (general) (CD3D, CD3E, and CD2) (K), B cell (CD19 and CD79A) (L), M1 Macrophage (NOS2 and PTGS2) (M), DCs (HLA-DPB1, HLA-DRA, HLA-DPA1, ITGAX, and CD1C) (N), Neutrophils (CD66b and CCR7) (O), Monocyte (CD86) (P), NK cell (KIR2DL3 and KIR3DL2) (Q), Th2 (STAT5A and IL13) (R), Treg (FOXP3, CCR8, STAT5B, and TGFβ) (S), Th1 (T-bet, STAT4, and IFN-γ) (T), T cell exhaustion (PD-1,CTLA4, LAG3, TIM-3, and GZMB) (U), and Tfh (BCL6 and IL21) (V).

Description	Gene markers	LUAD				LUSC			
		Normal		Tumor		Normal		Tumor	
		R	p	R	p	R	p	R	p
CD8+ T cell	CD8A	0.023	0.86	-0.061	0.18	-0.11	0.46	-0.18	***
T cell (general)	CD3D	-0.12	0.37	-0.14	**	-0.094	0.52	-0.24	***
	CD3E	-0.045	0.74	-0.16	***	-0.052	0.72	-0.21	***
	CD2	-0.11	0.41	-0.13	**	-0.073	0.61	-0.22	***
B cell	CD19	0.021	0.88	-0.27	***	0.054	0.71	-0.16	***
	CD79A	0.035	0.79	-0.28	***	-0.1	0.48	-0.19	***
Neutrophils	CD66b	0.029	0.83	-0.11	*	0.13	0.37	-0.1	*
	CCR7	0.081	0.54	-0.18	***	0.0036	0.98	-0.18	***
Dendritic cell	HLA-DPB1	0.17	0.2	-0.12	**	0.35	*	-0.13	**
	HLA-DQB1	-0.044	0.74	-0.11	*	-0.076	0.6	-0.083	0.067
	HLA-DRA	0.12	0.38	-0.091	*	0.22	0.13	-0.13	**
	HLA-DPA1	0.15	0.26	-0.071	0.12	0.056	0.27	-0.13	**
	CD1C	-0.12	0.38	-0.12	*	0.12	0.39	-0.072	0.11
	ITGAX	0.35	**	-0.037	0.42	0.3	*	-0.089	*
Th1	T-bet	-0.099	0.46	0.094	*	0.069	0.63	-0.21	***
	STAT4	-0.11	0.41	-0.002	0.97	-0.12	0.4	-0.083	**
	STAT1	0.0099	0.94	0.26	***	0.36	**	0.029	0.53
	IFN- γ	-0.17	0.2	0.057	0.21	-0.26	0.07	-0.12	**
Tfh	IL21	-0.008	0.95	0.026	0.56	0.043	0.77	-0.17	***
Th17	STAT3	0.14	0.29	0.11	*	0.3	*	0.16	***
Treg	FOXP3	0.15	0.25	-0.021	0.64	0.077	0.6	-0.12	**
	STAT5B	-0.054	0.69	-0.055	0.23	0.2	0.17	-0.092	*
	TGF β	0.46	***	0.17	***	0.53	***	0.33	***
T cell exhaustion	PD-1	0.082	0.54	0.011	0.82	0.069	0.63	-0.22	***
	CTLA4	0.032	0.81	-0.017	0.72	-0.092	0.53	-0.19	***
	LAG3	0.057	0.67	0.017	0.71	0.21	0.14	-0.14	**
	GZMB	-0.17	0.21	0.084	0.063	0.66	0.063	-0.17	***

Table 3. Correlation analysis between *PKM2* and marker genes of immune cells in GEPIA. * $p < 0.05$, ** $p < 0.01$, *** $p < 0.001$.

Materials and methods

PKM2 expression analysis

The Gent2 database (<http://gent2.appex.kr/gent2/>)³⁴, TIMER (<https://cistrome.shinyapps.io/timer/>), and GEPIA (<http://gepia.cancer-pku.cn/>) were used to investigate the mRNA expression levels of the *PKM2* in human cancers^{13,35}.

TIMER database

TIMER is a comprehensive web server for systematic analysis of immune infiltration in various cancer types³⁶. In this study, we used the “Diff Exp” module to study the expression difference of *PKM2* between tumors and adjacent normal tissues in diverse human cancers. The “Gene” module was used to explore the correlation of *PKM2* expression and the abundance of immune infiltrates, including B cells, CD8+ T cells, CD4+ T cells, macrophage, neutrophils and dendritic cells, in LUAD and LUSC. Furthermore, a correlation analysis was performed between *PKM2* expression and the expression of marker genes of infiltrating immune cells in LUAD and LUSC by the “Correlation” module¹³.

GEPIA database analysis

The GEPIA database, which incorporates RNA sequencing data from 9736 tumor tissues and 8587 normal tissues sourced from TCGA and the Genotype-Tissue Expression (GTEx) databases, was utilized in this study³⁷. Specifically, the “Boxplots” module of GEPIA was employed to analyze the expression of *PKM2* in various human cancers. The “Stage plot” module was used to investigate the relationship between *PKM2* expression and the pathological staging of LUAD and LUSC. Survival curves were generated using the “Survival Plots”, including OS and DFS, to assess the prognostic value of *PKM2*. The “correlation” module of the TIMER database was used to further validate the association between *PKM2* expression and specific markers of distinct immune cell subsets¹³.

Kaplan–Meier plotter

The data obtained from GEO, EGA and TCGA databases were analyzed using Kaplan Meier Plotter (<http://kmpplot.com/analysis/>) to evaluate the correlation between the expression of all genes and the patient survival in

more than 30,000 samples from 21 different tumor types³⁸. To specifically investigate the role of *PKM2* expression in lung cancer, gene chip dataset was used to analyze the correlation between *PKM2* expression and prognosis as well as various clinicopathological factors³⁹. The RNA-seq data was used to investigate the relationship between *PKM2* expression and the prognosis of LUAD and LUSC, including OS and RFS⁴⁰. Meanwhile, the expression levels of *PKM2* in tumor tissues and adjacent normal tissues were also compared by using the Kaplan–Meier plotter database⁴¹.

HPA

HPA (<https://www.proteinatlas.org>) database provides comprehensive proteomics, transcriptomics, and systems biology data⁴². The protein expression levels of *PKM2* in both tumor tissues and adjacent normal tissues of LUAD and LUSC patients were investigated using the HPA database.

PrognScan database

PrognScan (<http://dna00.bio.kyutech.ac.jp/PrognScan/PrognScan.html>) is a meta-analysis database for evaluating the prognostic value of genes⁴³. The associations between *PKM2* expression and clinical outcomes in 12 types of cancers were determined with a *p* value < 0.05 as the threshold using PrognScan³⁵.

Ethics statement

This study is based on summary data from public databases, which had gained written informed consent and ethics approval. No ethical approval is required for the secondary analysis of summary data.

Data availability

The datasets generated during the current study are available from the corresponding author on reasonable request.

Received: 9 October 2023; Accepted: 9 December 2023

Published online: 14 December 2023

References

- Sinha, A. *et al.* Early-stage lung adenocarcinoma MDM2 genomic amplification predicts clinical outcome and response to targeted therapy. *Cancers (Basel)* <https://doi.org/10.3390/cancers14030708> (2022).
- Howlader, N. *et al.* The effect of advances in lung-cancer treatment on population mortality. *N. Engl. J. Med.* **383**, 640–649. <https://doi.org/10.1056/NEJMoa1916623> (2020).
- Wang, C. *et al.* The heterogeneous immune landscape between lung adenocarcinoma and squamous carcinoma revealed by single-cell RNA sequencing. *Signal Transduct. Target Ther.* **7**, 289. <https://doi.org/10.1038/s41392-022-01130-8> (2022).
- Remark, R. *et al.* The non-small cell lung cancer immune contexture. A major determinant of tumor characteristics and patient outcome. *Am. J. Respir. Crit. Care Med.* **191**, 377–390. <https://doi.org/10.1164/rccm.201409-1671PP> (2015).
- Zhang, Z. *et al.* PKM2, function and expression and regulation. *Cell Biosci.* **9**, 52. <https://doi.org/10.1186/s13578-019-0317-8> (2019).
- Zhu, S. *et al.* Pyruvate kinase M2 (PKM2) in cancer and cancer therapeutics. *Cancer Lett.* **503**, 240–248. <https://doi.org/10.1016/j.canlet.2020.11.018> (2021).
- Wang, J. *et al.* Lactylation of PKM2 suppresses inflammatory metabolic adaptation in pro-inflammatory macrophages. *Int. J. Biol. Sci.* **18**, 6210–6225. <https://doi.org/10.7150/ijbs.75434> (2022).
- Gui, D. Y., Lewis, C. A. & Vander Heiden, M. G. Allosteric regulation of PKM2 allows cellular adaptation to different physiological states. *Sci. Signal* **6**, pe7. <https://doi.org/10.1126/scisignal.2003925> (2013).
- Liu, C., Liu, C. & Fu, R. Research progress on the role of PKM2 in the immune response. *Front. Immunol.* **13**, 936967. <https://doi.org/10.3389/fimmu.2022.936967> (2022).
- Chen, M., Liu, H., Li, Z., Ming, A. L. & Chen, H. Mechanism of PKM2 affecting cancer immunity and metabolism in tumor microenvironment. *J. Cancer* **12**, 3566–3574. <https://doi.org/10.7150/jca.54430> (2021).
- Xia, Q. *et al.* Tumor-associated macrophages promote PD-L1 expression in tumor cells by regulating PKM2 nuclear translocation in pancreatic ductal adenocarcinoma. *Oncogene* **41**, 865–877. <https://doi.org/10.1038/s41388-021-02133-5> (2022).
- Xu, C., Liu, W., Li, L., Wang, Y. & Yuan, Q. Serum tumour M2-pyruvate kinase as a biomarker for diagnosis and prognosis of early-stage non-small cell lung cancer. *J. Cell Mol. Med.* **25**, 7335–7341. <https://doi.org/10.1111/jcmm.16762> (2021).
- Gu, Y. *et al.* CCL14 is a prognostic biomarker and correlates with immune infiltrates in hepatocellular carcinoma. *Aging (Albany NY)* **12**, 784–807. <https://doi.org/10.18632/aging.102656> (2020).
- Mazurek, S. Pyruvate kinase type M2: A key regulator of the metabolic budget system in tumor cells. *Int. J. Biochem. Cell Biol.* **43**, 969–980. <https://doi.org/10.1016/j.biocel.2010.02.005> (2011).
- Bluemlein, K. *et al.* Pyruvate kinase is a dosage-dependent regulator of cellular amino acid homeostasis. *Oncotarget* **3**, 1356–1369. <https://doi.org/10.18632/oncotarget.730> (2012).
- Yu, W., Yang, Z., Huang, R., Min, Z. & Ye, M. SIRT6 promotes the Warburg effect of papillary thyroid cancer cell BCPAP through reactive oxygen species. *OncoTargets Ther.* **12**, 2861–2868. <https://doi.org/10.2147/ott.S194256> (2019).
- Damascono, L. E. A. *et al.* PKM2 promotes Th17 cell differentiation and autoimmune inflammation by fine-tuning STAT3 activation. *J. Exp. Med.* <https://doi.org/10.1084/jem.20190613> (2020).
- Luo, W. *et al.* Pyruvate kinase M2 is a PHD3-stimulated coactivator for hypoxia-inducible factor 1. *Cell* **145**, 732–744. <https://doi.org/10.1016/j.cell.2011.03.054> (2011).
- Yang, W. *et al.* Nuclear PKM2 regulates β -catenin transactivation upon EGFR activation. *Nature* **480**, 118–122. <https://doi.org/10.1038/nature10598> (2011).
- Hu, H. *et al.* The combination of PKM2 overexpression and M2 macrophages infiltration confers a poor prognosis for PDAC patients. *J. Cancer* **11**, 2022–2031. <https://doi.org/10.7150/jca.38981> (2020).
- Bian, Z. *et al.* LncRNA-FEZF1-AS1 promotes tumor proliferation and metastasis in colorectal cancer by regulating PKM2 signaling. *Clin. Cancer Res.* **24**, 4808–4819. <https://doi.org/10.1158/1078-0432.Ccr-17-2967> (2018).
- Xiao, H. *et al.* PKM2 promotes breast cancer progression by regulating epithelial mesenchymal transition. *Anal. Cell Pathol. (Amst.)* **8396023**, 2020. <https://doi.org/10.1155/2020/8396023> (2020).
- Li, T. E. *et al.* PKM2 drives hepatocellular carcinoma progression by inducing immunosuppressive microenvironment. *Front. Immunol.* **11**, 589997. <https://doi.org/10.3389/fimmu.2020.589997> (2020).

24. Verma, H., Cholia, R. P., Kaur, S., Dhiman, M. & Mantha, A. K. A short review on cross-link between pyruvate kinase (PKM2) and Glioblastoma Multiforme. *Metab. Brain Dis.* **36**, 751–765. <https://doi.org/10.1007/s11011-021-00690-y> (2021).
25. Wang, J. Z. *et al.* The role of the HIF-1 α /ALYREF/PKM2 axis in glycolysis and tumorigenesis of bladder cancer. *Cancer Commun. (Lond.)* **41**, 560–575. <https://doi.org/10.1002/cac2.12158> (2021).
26. Huang, Y. *et al.* HIF-1 α switches the functionality of TGF- β signaling via changing the partners of smads to drive glucose metabolic reprogramming in non-small cell lung cancer. *J. Exp. Clin. Cancer Res.* **40**, 398. <https://doi.org/10.1186/s13046-021-02188-y> (2021).
27. Hua, Q. *et al.* Hypoxia-induced lncRNA-AC020978 promotes proliferation and glycolytic metabolism of non-small cell lung cancer by regulating PKM2/HIF-1 α axis. *Theranostics* **10**, 4762–4778. <https://doi.org/10.7150/thno.43839> (2020).
28. Zhou, S. *et al.* Hypoxic tumor-derived exosomes induce M2 macrophage polarization via PKM2/AMPK to promote lung cancer progression. *Cell Transplant.* **31**, 9636897221106998. <https://doi.org/10.1177/09636897221106998> (2022).
29. Mao, X. *et al.* Crosstalk between cancer-associated fibroblasts and immune cells in the tumor microenvironment: New findings and future perspectives. *Mol. Cancer* **20**, 131. <https://doi.org/10.1186/s12943-021-01428-1> (2021).
30. Hou, P. P. *et al.* Ectosomal PKM2 promotes HCC by inducing macrophage differentiation and remodeling the tumor microenvironment. *Mol. Cell* **78**, 1192–1206.e1110. <https://doi.org/10.1016/j.molcel.2020.05.004> (2020).
31. Lei, X. *et al.* Immune cells within the tumor microenvironment: Biological functions and roles in cancer immunotherapy. *Cancer Lett.* **470**, 126–133. <https://doi.org/10.1016/j.canlet.2019.11.009> (2020).
32. Pardoll, D. M. The blockade of immune checkpoints in cancer immunotherapy. *Nat. Rev. Cancer* **12**, 252–264. <https://doi.org/10.1038/nrc3239> (2012).
33. Stirling, E. R. *et al.* Metabolic implications of immune checkpoint proteins in cancer. *Cells* <https://doi.org/10.3390/cells11010179> (2022).
34. Park, S. J., Yoon, B. H., Kim, S. K. & Kim, S. Y. GENT2: An updated gene expression database for normal and tumor tissues. *BMC Med. Genom.* **12**, 101. <https://doi.org/10.1186/s12920-019-0514-7> (2019).
35. Tuo, Z. *et al.* RUNX1 is a promising prognostic biomarker and related to immune infiltrates of cancer-associated fibroblasts in human cancers. *BMC Cancer* **22**, 523. <https://doi.org/10.1186/s12885-022-09632-y> (2022).
36. Li, T. *et al.* TIMER: A web server for comprehensive analysis of tumor-infiltrating immune cells. *Cancer Res.* **77**, e108–e110. <https://doi.org/10.1158/0008-5472.Can-17-0307> (2017).
37. Tang, Z. *et al.* GEPIA: A web server for cancer and normal gene expression profiling and interactive analyses. *Nucleic Acids Res.* **45**, W98–W102. <https://doi.org/10.1093/nar/gkx247> (2017).
38. Györfy, B. Discovery and ranking of the most robust prognostic biomarkers in serous ovarian cancer. *Geroscience* **45**, 1889–1898. <https://doi.org/10.1007/s11357-023-00742-4> (2023).
39. Györfy, B., Surowiak, P., Budczies, J. & Lánckzy, A. Online survival analysis software to assess the prognostic value of biomarkers using transcriptomic data in non-small-cell lung cancer. *PLoS ONE* **8**, e82241. <https://doi.org/10.1371/journal.pone.0082241> (2013).
40. Nagy, Á., Munkácsy, G. & Györfy, B. Pancancer survival analysis of cancer hallmark genes. *Sci. Rep.* **11**, 6047. <https://doi.org/10.1038/s41598-021-84787-5> (2021).
41. Bartha, Á. & Györfy, B. TNMplot.com: A web tool for the comparison of gene expression in normal, tumor and metastatic tissues. *Int. J. Mol. Sci.* <https://doi.org/10.3390/ijms22052622> (2021).
42. Asplund, A., Edqvist, P. H., Schwenk, J. M. & Pontén, F. Antibodies for profiling the human proteome: The Human Protein Atlas as a resource for cancer research. *Proteomics* **12**, 2067–2077. <https://doi.org/10.1002/pmhc.201100504> (2012).
43. Mizuno, H., Kitada, K., Nakai, K. & Sarai, A. PrognosScan: A new database for meta-analysis of the prognostic value of genes. *BMC Med. Genom.* **2**, 18. <https://doi.org/10.1186/1755-8794-2-18> (2009).

Author contributions

All authors contributed to the study and conception and design. Material preparation, data collection and analysis were performed by L.Y. and J.S.. The first draft of the manuscript was written by L.Y. and all authors commented on previous versions of the manuscript. All authors read and approved the final manuscript.

Funding

This work was supported by the National Natural Science Foundation of China (Grant Number: 31970698) and the Sichuan Science and Technology Program (Grant Number: 2023YFS0109).

Competing interests

The authors declare no competing interests.

Additional information

Supplementary Information The online version contains supplementary material available at <https://doi.org/10.1038/s41598-023-49558-4>.

Correspondence and requests for materials should be addressed to Y.M.

Reprints and permissions information is available at www.nature.com/reprints.

Publisher's note Springer Nature remains neutral with regard to jurisdictional claims in published maps and institutional affiliations.



Open Access This article is licensed under a Creative Commons Attribution 4.0 International License, which permits use, sharing, adaptation, distribution and reproduction in any medium or format, as long as you give appropriate credit to the original author(s) and the source, provide a link to the Creative Commons licence, and indicate if changes were made. The images or other third party material in this article are included in the article's Creative Commons licence, unless indicated otherwise in a credit line to the material. If material is not included in the article's Creative Commons licence and your intended use is not permitted by statutory regulation or exceeds the permitted use, you will need to obtain permission directly from the copyright holder. To view a copy of this licence, visit <http://creativecommons.org/licenses/by/4.0/>.

© The Author(s) 2023